A Low-Voltage and Low-Power RF MEMS Series and Shunt Switches Actuated by Combination of Electromagnetic and Electrostatic Forces

Il-Joo Cho, Taeksang Song, Sang-Hyun Baek, and Euisik Yoon, *Member, IEEE*

Abstract—This paper reports new RF microelectromechanical systems (MEMS) switches actuated by the combination of electromagnetic and electrostatic forces for low-voltage and low-power operation. The proposed RF MEMS switches have utilized the proper combination of two actuation mechanisms: taking advantage of the large actuation force from electromagnetic actuation for initial movement and the low-power feature from electrostatic actuation for holding the actuator position. Both series- and shunt-type switches have been implemented using the proposed actuation mechanism. From the fabricated switches, feasibility of operation has been successfully demonstrated. The fabricated switches can be operated within several hundred microseconds. In the series-type switch, the isolation has been measured as −34 dB and insertion loss as −0.37 dB at 20 GHz. In the shunt type switch, the isolation is −20.7 dB and insertion loss is −0.85 dB at 19.5 GHz. The proposed RF MEMS switches are mechanically robust and the combination of electromagnetic and electrostatic actuations makes it possible to achieve excellent switching characteristics at low power and low voltage below 5 V.

Index Terms—Electromagnetic actuation, electrostatic actuation, RF microelectromechanical systems (MEMS) switch, series type, shunt type.

I. INTRODUCTION

WIRELESS communication has made an explosive growth of emerging consumer markets, as well as in military applications of RF, microwave, and millimeter-wave circuits and systems. These include wireless personal communication systems, wireless local area networks, satellite communications, automotive electronics, etc. In these systems, the RF switch is one of the essential components to handle RF signals [1]. Previously, RF switching has been implemented by using p-i-n diodes and GaAs MESFETs in the form of junction field-effect transistor (JFET)-based semiconductor switches [2], [3]. However, these semiconductor switches show poor performance in the respect of signal loss and power consumption as the frequency increases. Recently, RF microelectromechanical systems (MEMS) switches have been introduced for low

insertion loss, high isolation, and low power consumption [4], [5].

Most of the RF MEMS switches reported to date have used electrostatic actuation [6]–[9]. Electrostatic actuation offers extremely low-power consumption and easy implementation. However, there are two main challenging issues to be addressed for the RF MEMS switches actuated by electrostatic force: high actuation voltage and low mechanical stability. The high actuation voltage degrades life time and often induces malfunction by the charge trapping problem. In order to lower the actuation voltage, meander spring-type [10] and push–pull concepts have been investigated [11]. The meander spring-type approach has a tradeoff between switching speed and spring constant, while the push–pull concept needs a still high actuation voltage compared to other actuation alternatives such as piezoelectric or Lorentz force actuation. Small electrostatic force still makes it difficult for the switches to be mechanically robust and to provide high isolation due to the restriction imposed on the maximum initial gap.

By using electromagnetic force actuation, the above problems can be resolved. Large force exerted from electromagnetic actuation allows RF switches to have a mechanically robust structure because they can be implemented with a high spring-constant membrane. Electromagnetic actuation force is also independent of initial actuator positions and exerts constant force regardless of the amount of displacement. Therefore, the switches can achieve high isolation from a large initial gap. Furthermore, the device can be operated with lower actuation voltage and have a longer life time. However, electromagnetic actuation requires relatively large power because constant current has to be applied during a given switching period [12]. Previously reported electromagnetically actuated switch requires large area and is difficult to be used in an array because a coil is fabricated on the bottom layer [13].

In this paper, we have proposed a new low-voltage and low-power RF MEMS switch actuated by the combination of electromagnetic and electrostatic forces with a latching mechanism [14], [15]. It is actuated by large electromagnetic force with low voltage and maintained its states by electrostatic force with low-power consumption. This combined actuation allows the proposed RF MEMS switch to be operated at low voltage, as well as low-power consumption. There are two types of RF MEMS switches: series type and shunt type. These two types of switches have their unique features and specific applications according to the frequency range. In this study, we have implemented both types using the proposed actuation mechanism.
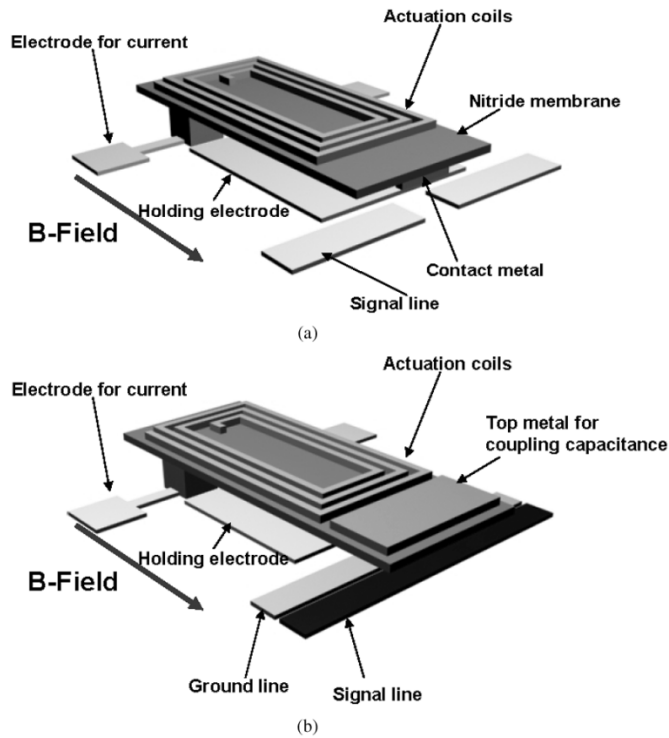
Fig. 1. Schematic diagram of the proposed RF MEMS switches. (a) Series-type switch. (b) Shunt-type switch.

II. STRUCTURES AND OPERATION

The proposed RF MEMS switch structures are shown in Fig. 1. Fig. 1(a) represents the series-type RF MEMS switch and Fig. 1(b) represents the shunt-type RF MEMS switch, respectively. The structure of the series-type switch is similar to that of the shunt-type switch, except for signal lines and the associated contact metal configuration. The switching structure consists of the two parts: a cantilever membrane integrated with coils for electromagnetic actuation and a bottom electrode for electrostatic actuation. The bottom electrode is used for electrostatic holding of the membrane when the membrane is deflected to touch the bottom electrode. Signal paths are formed in coplanar waveguide (CPW) lines under the movable cantilever. The initial gap between the cantilever membrane and the bottom signal lines is determined from the process condition. The membrane structure is mechanically connected to the bottom plane via anchors, as well as for electrical connections. The actuation coils on the membrane are connected to the bottom metal layer to apply an actuation current. In the case of the series-type switch, there is a contact metal located at the end of the membrane and the CPW line on the bottom layer is cut off to isolate the signal. Initially, the switch is in the "off" state. When the membrane is actuated downward, the contact metal connects the broken CPW line and the switching state changes to the "on" state. In the case of the shunt-type switch, however, there is a top metal plane at the end of the membrane and the CPW line on the bottom layer is initially connected. The initial state of the shunt-type switch is "on" and it changes its state to "off" when the membrane is actuated downward. During the "off" state, the top metal layer forms capacitance coupling
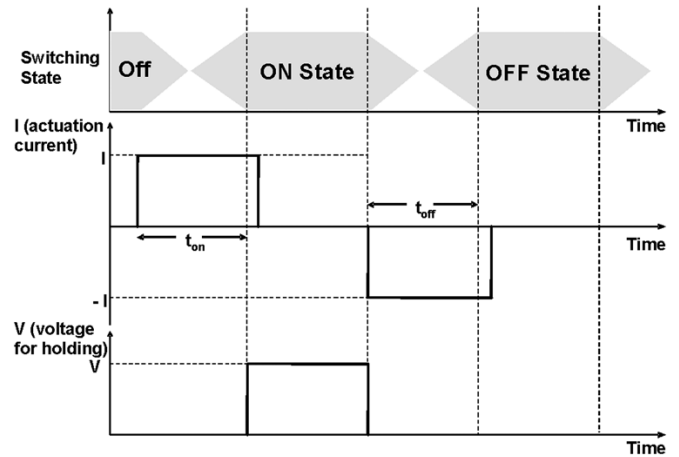

Fig. 2. Timing diagram of control signals for switching operation.

between the signal and ground lines through the membrane as a dielectric layer. From this capacitive coupling, the input RF signal is bypassed to the ground instead of being transmitted to the output port. As a result, the switch is turned off.

Fig. 2 shows the timing diagram of the proposed series-type switch according to its switching state and control signals. Initially, the contact metal is detached from the signal line by an initial gap. When an external current is applied to the coil counterclockwise, the membrane is actuated downward by Lorentz force and the contact metal makes an electrical connection to the underlying CPW signal line. After that, electrostatic force between the coils and the bottom electrode is activated to hold the membrane, maintaining its "on" state without static power consumption. For switching its state back to the "off" state, a current should be applied clockwise and then the contact metal is detached from the bottom signal line by Lorentz force, as well as mechanical restoring force. This large restoring force enables the contact metal to be easily detached from the bottom metal with less risk of stiction to the signal lines while the RF signal is being applied, i.e., so-called hot switching. This hot-switching stiction is known to be due to a microwelding effect and may make the switch permanently closed. This actually gives a significant impact on the power-handling capability of the switch. It has been observed that the microwelding occurs typically at signal power levels greater than 20 dBm [16], [17]. Therefore, the large restoring force of the proposed switches can allow improved power-handling capabilities. The timing diagram of the shunt-type switch is identical to that of the series type, except that switching states are reversed.

As explained above, the proposed switch changes its states by large electromagnetic force and holds its state with electrostatic force. The electromagnetic actuation force is constant regardless of an initial height of the membrane from the bottom plane. This allows a large initial gap and high signal isolation. We can also achieve high power-handling capability from the large restoring force and high immunity to vibration due to the high spring constant structure. In addition, operation voltage can be maintained below 5 V because the electrostatic force is only applied during the holding state when an extremely small gap is already formed between the bottom electrode and coils. On
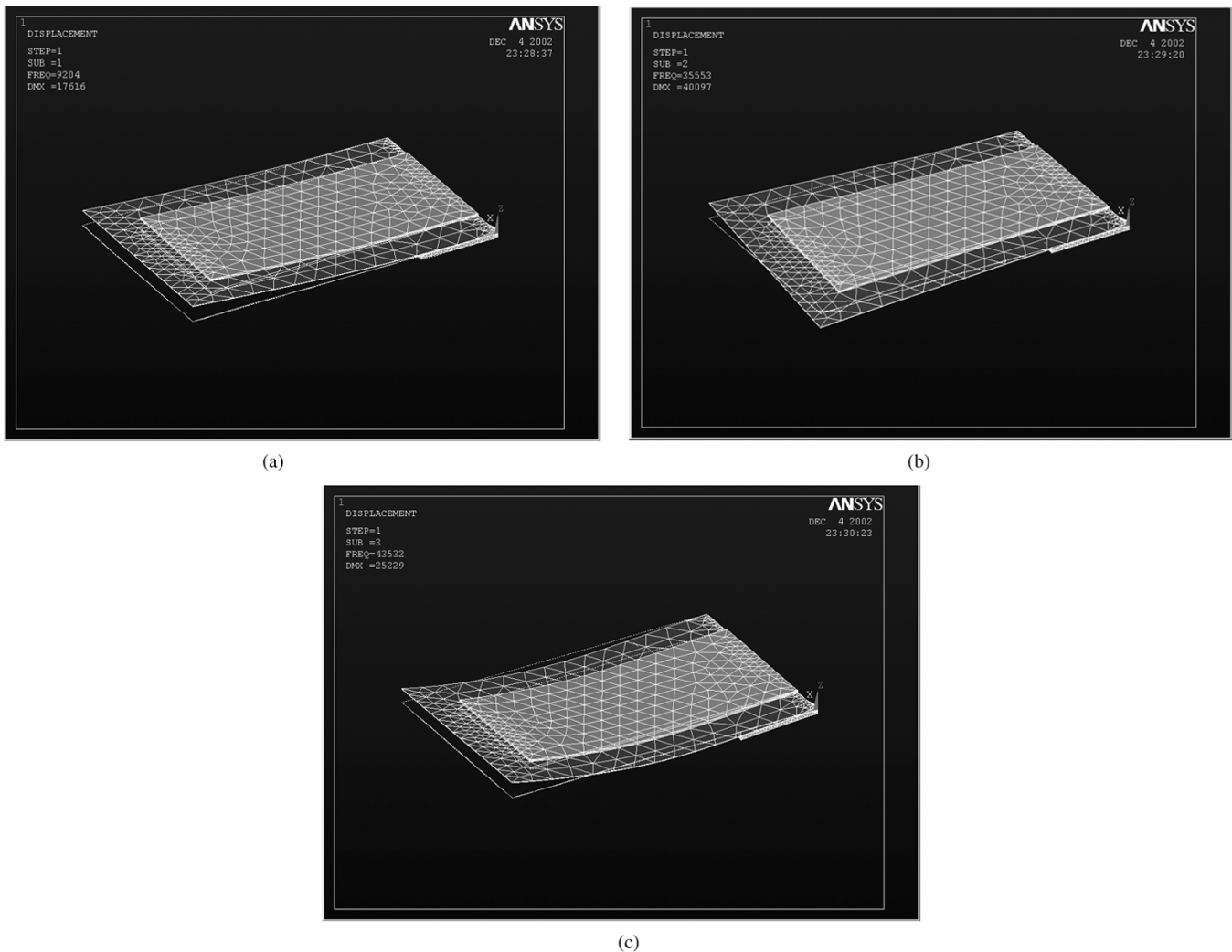
Fig. 3. Mechanical resonant frequencies from FEM simulation results using ANSYS. (a) First mode. (b) Second mode. (c) Third mode.

the contrary, electromagnetic force is only required during the short period of time for switching its state. Therefore, the proposed switches can operate at low voltage, as well as low-power consumption.

III. DESIGN AND SIMULATIONS

Design optimizations of the proposed switches are performed by finite-element method (FEM) simulation using ANSYS. The mechanical characteristics of series- and shunt-type switches are similar, and a simplified model has been used to simulate their mechanical characteristics. To optimize and determine the dimensions of the structure, some selected mechanical characteristics have been considered such as actuation voltage, spring constant, resonant frequency, switching time, and initial gap. With an external magnetic field of 0.22 T, electromagnetic force is calculated to be approximately 20 μN with an effective coil length of 1.86 mm and an actuation current of 50 mA. With this electromagnetic force, mechanical displacement has been predicted by using ANSYS. Simulated displacement is 13.6 μm, and this result shows that the exerted electromagnetic force is large enough to actuate the proposed switch more than 10 μm,

which is the initial height for the initial prototype design. Resonant frequencies have also been simulated from dynamic simulation modes, as shown in Fig. 3. The first mode resonant frequency is 9.2 kHz, and the second and third modes are 35.6 and 43.5 kHz, respectively. The operational actuation mode is the first mode, and these results guarantee stable operation because the second and third mode resonant frequencies are far from the operation mode. The switching time inferred from the simulation is 275 μs. From the switching time obtained from mechanical simulations, power consumption can be estimated. The proposed RF MEMS switch consumes power only during the time when the switch changes its states from "off" to "on" or "on" to "off." The estimated power consumption is approximately 140 μJ per each switching cycle. Table I summarizes the dimensions of the proposed switch determined from simulations.

IV. FABRICATION

Fabrication processes of the proposed MEMS switches are shown in Fig. 4. The fabrication process of the series- and shunt-type switches are compatible with each other. However, the fabrication process of the shunt-type switch can be simpler than

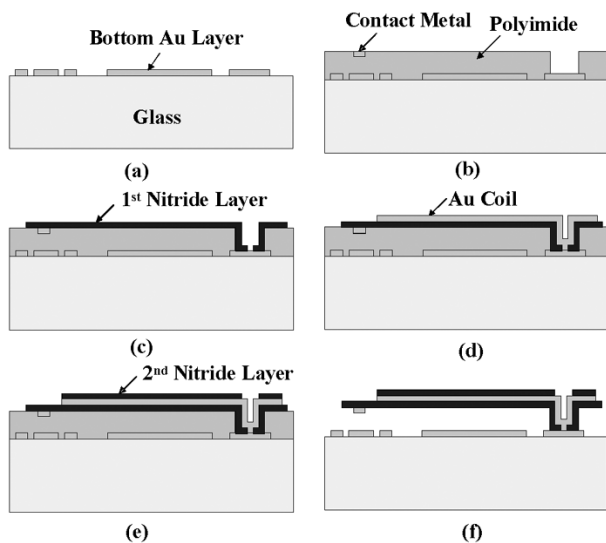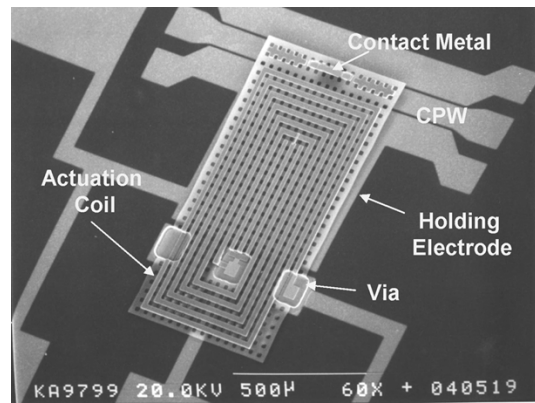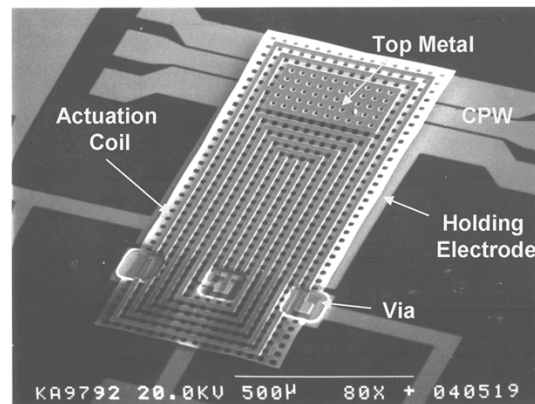|	
Cantilever width	500μm
Cantilever length	700μm
Cantilever thickness	1μm
Coil width	20μm
Coil spacing	10μm
Coil thickness	3μm
Effective area of electrode	320μm x 450μm
Initial gap	10μm
Spring constant	12N/m
Restoring force	140μN

Fig. 4. Fabrication process flow. (a) Bottom metal layer deposition. (b) Polyimide sacrificial layer patterning and contact metal liftoff. (c) First nitride layer deposition and patterning. (d) Gold coil electroplating. (e) Second nitride layer deposition and patterning. (f) Sacrificial layer removal.

Fig. 5. Scanning electron microscopy (SEM) photograph of the fabricated switches with CPW signal lines. (a) Series-type switch. (b) Shunt-type switch.

that of the series-type switch because the contact metal deposition process is not required for the shunt-type switch. In general, the two types of switches can be simultaneously fabricated on the single wafer. The process flow is as follows. A glass wafer is chosen as a starting material to reduce the substrate loss of RF signals. First, Cr/Au is deposited for CPW signal lines and bottom electrodes using a liftoff process, as shown in Fig. 4(a). A 10-μm-thick polyimide is then spun and cured for a sacrificial layer. The thickness of this polyimide film is very important because it determines the initial height of the membrane, which influences the isolation of the series-type switch during the "off" state and the insertion loss of the shunt type switch during the "on" state. The cured polyimide is patterned twice using reactive ion etching (RIE) with aluminum as a mask. First, a shallow etch is performed to produce a recessed area for the contact metal to enhance contact characteristics. After that, a deep etch is performed for the formation of anchors, which connect torsion bars to the bottom metal electrically and mechanically.

Next, Au/Cr is deposited using a liftoff process for contact metal, as shown in Fig. 4(b). Chrome is used for an adhesion layer between the nitride and Au layers. The first plasma-enhanced chemical vapor deposition (PECVD) silicon–nitride layer is then deposited and patterned for the membrane, as shown in Fig. 4(c). The deposited film thickness is minimized to be approximately 200 nm to obtain a low holding voltage because this nitride film thickness determines the electrostatic force at the holding stage of the fabricated RF MEMS switch. After patterning the first nitride layer, Cr/Au is deposited for a seed metal for electroplating gold coils about 3 μm using AZ9260 as a mold, as shown in Fig. 4(d).

Next, the AZ9260 mold is removed and the second nitride layer of 600 nm is deposited and patterned [see Fig. 4(e)]. This second nitride layer plays an important role in releasing the residual stress of the membrane. The membrane is composed of three layers, i.e., the first nitride layer, an electroplated gold layer, and the second nitride layer. This sandwich film compensates for the stress on each other and a stress-free membrane can be obtained, as shown in Fig. 5. The total thickness of the membrane is approximately 3.8 μm thick and this thick structure can enhance the mechanical stability. Finally, a sacrificial layer is removed using a barrel asher and the membrane is released, as shown in Fig. 4(f).

The fabricated MEMS switches, both the series and shunt types, are shown in Fig. 5. This figure shows that the stress of the membrane has been compensated and the membranes
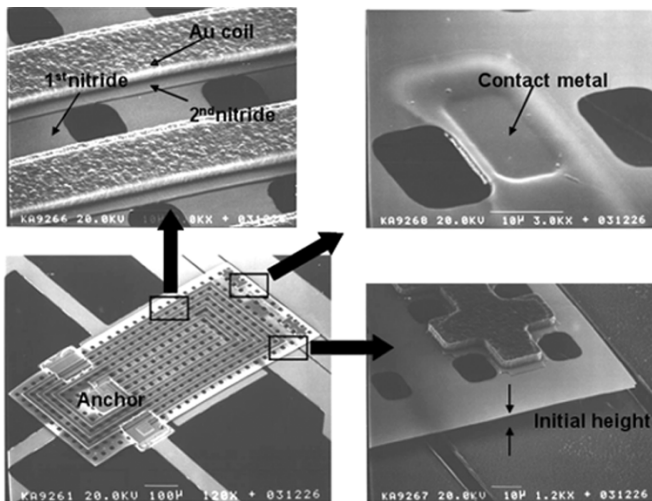
Fig. 6.   Enlarged view of the fabricated MEMS switches.

Fig. 7.   Experimental setup for measuring mechanical characteristics of the fabricated RF MEMS switches.

are almost stress free. There are two control signal lines for actuation of the fabricated switches: one for actuation and the other for holding. At the end of the membrane, contact metal is formed for the series-type switch, while the top metal layer is formed for the shunt-type switch. Actuation coils are connected to the bottom metal lines through vias. Fig. 6 shows the enlarged view of the fabricated switches. The etch holes on the membrane helps the polyimide removal in short time. The distance between the bottom electrode and membrane has been approximately 10.5 μm in the series type and approximately 12.5 μm in the shunt type, respectively. The slight difference in the height comes from upward bending in the membrane of the shunt-type switch due to the stress induced by the additional top electrode layer. This initial height is approximately four times larger than that of the previously reported ones [10], [11]. The gold coil area in the membrane has been maximized to reduce the holding voltage by enlarging the effective area for electrostatic force.

V. MEASUREMENT RESULTS AND DISCUSSION

A. Mechanical Characteristics

The fabricated MEMS series- and shunt-type switches have been actuated by electromagnetic force induced on the coils from external permanent magnets. To apply an external magnetic field, the diced RF MEMS switch is fixed on a printed circuit board (PCB) and wire bonded and is inserted between the two permanent magnets. External magnetic intensity is 0.22 T (or 2200 G) at the actuation point.

Mechanical characteristics of the fabricated switch have been measured using Polytec's laser Doppler vibrometer (LDV). Fig. 7 shows the experimental setup for measuring mechanical characteristics. Displacement of the actuated series-type switch is measured as a function of applied current, as shown in Fig. 8. The shunt-type switch has a similar result. The displacement is quite linear, confirming the general property of electromagnetic actuation. One of the big advantages of magnetic actuation for RF switch applications is that its actuation force is constant and is not a function of the gap between the two electrodes. This constant force can reduce a possible mechanical damage to the
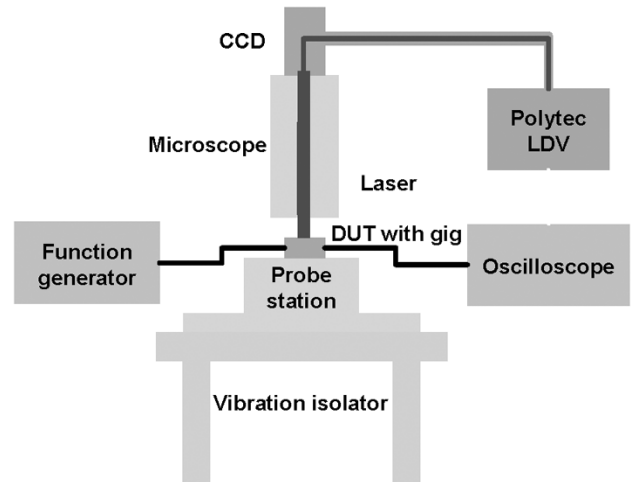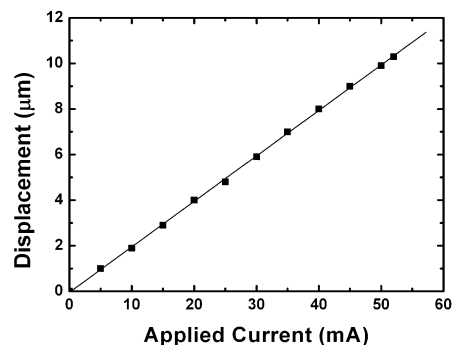

Fig. 8.   Displacement of the fabricated series-type switch as a function of applied actuation current.

contact metals at the moment of switching, which is a serious problem in the case of electrostatic actuation. In electrostatic actuation, the force increases inversely proportional to the square of the gap between two contact metals. Therefore, the contact metals experience an accelerated mechanical impulse shock at the moment of contact. With an applied current of 53 mA, we can successfully actuate the switch to the "on" state. The resistance of coil is 38 Ω. The corresponding maximum actuation voltage is 2.0 V and the applied force is estimated as 25.2 μN from the applied magnetic-field intensity. The maximum displacement of the series type switch is 10.5 μm and a spring constant of the fabricated cantilever has been calculated to be 2.4 N/m. The holding voltage for maintaining its state has been measured below 3.7 V. Table II summarized the mechanical properties of the fabricated series- and shunt-type switches. The spring constant of the shunt type is slightly lower than that of the series type because the length of membrane is longer by approximately 50 μm.

The switching time and power consumption have been estimated from dynamic response of the fabricated switches, as shown in Fig. 9. Fig. 9(a) shows the frequency response and Fig. 9(b) shows the transient response of the fabricated series-type switch. Form the frequency response, resonant frequency of the fabricated series-type switch can be directly obtained to be 4.5 kHz. The dynamic transient response of the switch

TABLE II
SUMMARY OF MECHANICAL AND ELECTRICAL CHARACTERISTICS
OF THE FABRICATED MEMS SWITCHES

	Series type	Shunt type
Applied Current	53mA	49mA
Coil Resistance	38Ω	46Ω
Applied Voltage	2.0V	2.3V
Holding Voltage	3.7V	3.3V
Initial Height	10.5μm	12.5μm
Spring Constant	2.4N/m	2.0N/m
Resonance Frequency	4.5kHz	2.2kHz
Switching time (on to off)	110μs	780μs
Switching time (off to on)	380μs	230μs
Energy for Switching	40.3μJ	87.9μJ
Contact Resistance	0.5Ω	---

Fig. 10.   Measured RF characteristics of the fabricated series-type switch. (a) Isolation for the "off" state. (b) Insertion loss for the "on" state.

to "off" in a half period of the resonant frequency. This can be guaranteed as long as the distance between the membrane and the bottom layer is large enough to give high isolation during the rest of the transient time. When the switch changes its state from "off" to "on," several periods are required to completely change its state due to the bounding from the bottom electrode after touching. From the dynamic response, the switching time can be estimated to be 110 μs for the transition from the "on" to the "off" state and 380 μs for the transition from the "off" to the "on" state, respectively. The resonant frequency of the shunt-type switch is lower by approximately 10% than that of the series type because the mass is larger and the spring constant is lower than that of the series type.

Power consumption of the fabricated switch can be calculated from the switching time. The switch consumes power only during the time that it changes its states. From the switching time of 380 μs, the required energy for switching is estimated as 40.3 μJ, which is lower than previous magnetic switch [13]. DC contact resistance has been measured using deembedding patterns. The measured contact resistance is 0.5 Ω during the "on" state and the "off" state resistance between two ports is infinite, as expected.

B. RF Characteristics

The RF characteristics of the fabricated series- and shunt-type RF MEMS switches have been measured using an HP network analyzer. External electrical control signals are applied on the fabricated switch for actuation and *s*-parameters of the input and output ports are extracted using a network analyzer. Fig. 10 shows the measured RF characteristics of the series-type switch. The isolation represents the performance of the switch in the "off" state. The isolation value has been measured from $S21$ parameters when the contact metal is detached from the bottom signal lines. The measured isolation is −61 dB at 2 GHz and
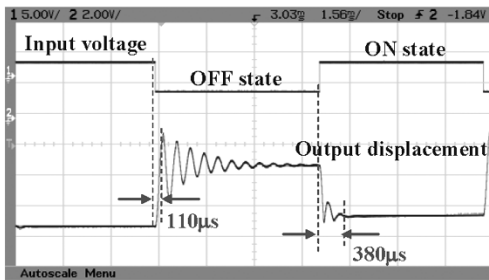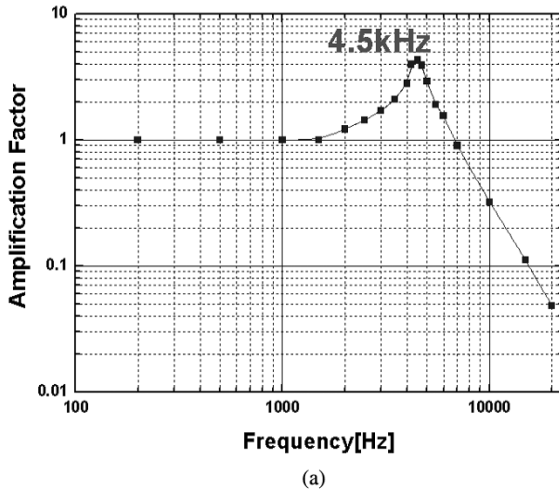

Fig. 9.   (a) Frequency response of the fabricated series-type switch. (b) Transient response of the fabricated series-type switch.

has been measured with a rectangular wave input signal. Resonant frequency can also be estimated from the transient response. When the switch changes its state from the "on" state (membrane down) to the "off" state (membrane up) in the series-type switch, the membrane oscillates with a resonant frequency. From Fig. 9(b), the switch changes its state from "on"
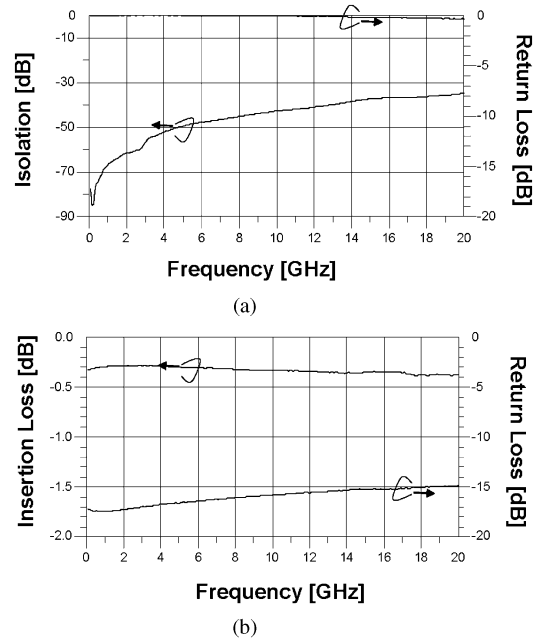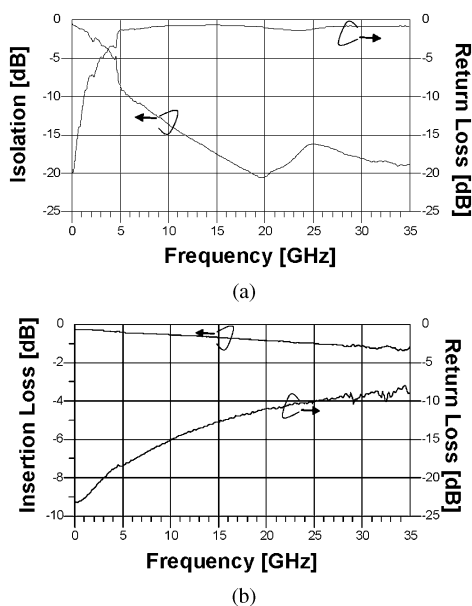
Fig. 11. Measured RF characteristics of the fabricated shunt-type switch. (a) Isolation for the "off" state. (b) Insertion loss for the "on" state.

-34 dB at 20 GHz, respectively. This large isolation can be achieved thanks to the high initial gap between the signal lines and contact metal. During the "off" state, the main source of signal coupling from the input to output port is the parasitic capacitance between the cutoff signal lines and contact metal. In the fabricated RF MEMS switch, the coupling capacitance is less than 1.2 fF, which is small enough to obtain large isolation from the high initial gap of 10.5 μm. Insertion loss has been characterized by using $S21$ parameters for the "on" state. The insertion loss is measured as -0.28 dB at 2 GHz and -0.37 dB at 20 GHz, respectively. The signal loss in the long CPW lines is subtracted from the measured insertion loss in order to extract the signal loss only in the contact switch metal.

Fig. 11 shows the measured RF characteristics of the shunt-type switch. The operation frequency of the shunt-type switch is typically higher than that of the series type. Therefore, the RF characteristics of the fabricated shunt-type RF MEMS switch are measured for the extended frequency range up to 35 GHz. The shunt-type switch is initially in the "on" state. The insertion loss measured during the "on" state denotes parasitic signal loss from coupling to the ground and it increases as frequency goes up. The insertion loss of the switch is characterized by measuring $S21$ parameters through the input and output terminals in the "on" state with no electrical control signal. The measured insertion loss is -0.85 dB at 19.5 GHz and -1.32 dB at 35 GHz, respectively. The insertion loss is mainly determined by the signal coupling to the ground and the CPW line loss. In the fabricated switch, the coupling loss is very low due to low coupling capacitance in the "on" state thanks to a large initial height of 12.5 μm. However, the CPW loss is relatively large compared to the previously reported ones [18], [19]. This is because the long ($\sim$1 mm) and thin (500 nm) CPW lines are used. To reduce the insertion loss, the CPW line loss should be reduced.

Isolation represents the performance of the "off" state and has been measured with $S21$ parameters along the signal lines

with the cantilever actuated downward. High isolation can be achieved by large coupling capacitance between the signal and ground lines through the top metal. This coupling capacitance change of the shunt-type switch is determined by the change of the overlap area and gap between the top metal and signal lines. The coupling capacitance ratio of the "off" state to the "on" state is approximately 62.5. The maximum isolation is measured as -20.7 dB at 19.5 GHz. At this frequency, a series resonance occurred due to the parasitic inductance incurred by the top metal layer. The resonance frequency can be adjusted by varying this parasitic inductance. However, the measured isolation value is smaller than expected. The main reason for this is considered that good physical contact has not been made between the bottom metal lines and the membrane due to some residues left over after removing the polyimide sacrificial layer.

VI. CONCLUSIONS

In this paper, we have proposed new low-voltage and low-power RF MEMS switches actuated by the combination of electromagnetic and electrostatic forces. The proposed switch uses electromagnetic force only during switching transition periods and, for the rest of the holding period, it uses electrostatic force to maintain low-power consumption. We have successfully implemented both series- and shunt-type RF MEMS switches using the proposed actuation scheme. From the large electromagnetic force, which is independent of initial actuator positions, the proposed RF MEMS switches can allow a large gap between the actuator and signal lines. From this, we can achieve high isolation in the "off" state for the series-type switch and low insertion loss in the "on" state for the shunt-type switch. Also, large electromagnetic force can provide a mechanically robust structure to guarantee reliable operation. Furthermore, large restoring force can increase power-handling capability of the fabricated switches by using bidirectional magnetic force. The fabricated switches show the maximum actuation voltage below 3.7 V and the maximum power consumption less than 87.9 μJ per switching. The series-type switch gives isolation of -34 dB and insertion loss of -0.37 dB at 20 GHz, respectively. The shunt-type switch shows isolation of -20.7 dB and insertion loss of -0.85 dB at 19.5 GHz, respectively.

It is expected that there is an ample room to improve performance through optimization of design and fabrication. The mechanically robust structure can guarantee stable operation and extend lifetime of the fabricated switches. In addition to that, small actuation voltage will make it easy to be integrated with other components and extends its possibility to CMOS integration as a viable SoC solution for future wireless communication products.

REFERENCES

[1] H. A. C. Tilmans, W. D. Raedt, and E. Beyne, "MEMS for wireless communications," *J. Micromech. Microeng.*, vol. 13, pp. 139–163, Jun. 2003.

[2] L. W. Ke, Y. J. Chan, and Y. C. Chiang, "Monolithic microwave Al-GaAs/InGaAs doped-channel FET switches," *Microwave Opt. Technol. Lett.*, vol. 13, no. 1, pp. 47–49, Sep. 1996.

[3] K. Kawakyu, Y. Ikeda, M. Nagaoka, and N. Uchitomi, "A novel resonant-type GaAs SPDT switch IC with low distortion characteristics for 1.9 GHz personal handy-phone system," in *IEEE MTT-S Int. Microwave Symp. Dig.*, San Francisco, CA, Jun. 1996, pp. 647–650.

[4] G. M. Rebeiz and J. B. Muldavin, "RF MEMS switches and switch circuits," *IEEE Micro*, vol. 2, pp. 59–71, Dec. 2001.

[5] E. R. Brown, "RF-MEMS switches for reconfigurable integrated circuits," *IEEE Trans. Microw. Theory Tech.*, vol. 46, no. 11, pp. 1868–1880, Nov. 1998.

[6] S. P. Pacheco, L. P. B. Katehi, and C.-T. Nguyen, "Design of low actuation voltage RF MEMS switch," in *IEEE MTT-S Int. Microwave Symp. Dig.*, Boston, MA, Jun. 2000, pp. 165–168.

[7] S.-C. Shen and M. Reng, "Low actuation voltage RF MEMS switches with signal frequencies from 0.25 GHz to 40 GHz," in *IEEE Electron Devices Meeting*, Washington, DC, Dec. 1999, pp. 689–692.

[8] J. Y. Park, G. H. Kim, K. W. Chung, and J. U. Bu, "Electroplated RF MEMS capacitive switches," in *Proc. IEEE MEMS Conf.*, Miyazaki, Japan, Jan. 2000, pp. 639–644.

[9] D. Peroulis, S. Pacheco, K. Sarabandi, and L. P. B. Katehi, "MEMS devices for high isolation switching and tunable filtering," in *IEEE MTT-S Int. Microwave Symp. Dig.*, Boston, MA, Jun. 2000, pp. 1217–1220.

[10] S. P. Pacheco, L. P. B. Katehi, and C.-T. Nguyen, "Design of low actuation voltage RF MEMS switch," in *IEEE MTT-S Int. Microwave Symp. Dig.*, Boston, MA, Jun. 2000, pp. 165–168.

[11] D. Hah, E. Yoon, and S. Hong, "A low voltage actuated micromachined microwave switch using torsion springs and leverage," in *IEEE MTT-S Int. Microwave Symp. Dig.*, Boston, MA, Jun. 2000, pp. 157–160.

[12] W. P. Taylor, O. Brand, and M. G. Allen, "Fully integrated magnetically actuated micromachined relays," *J. Microelectromech. Syst.*, vol. 7, pp. 181–191, Jun. 1998.

[13] M. Ruan, J. Shen, and C. B. Wheeler, "Latching micromagnetic relays," *J. Microelectromech. Syst.*, vol. 10, no. 6, pp. 511–517, Dec. 2001.

[14] I.-J. Cho, K.-S. Yun, H.-K. Lee, J.-B. Yoon, and E. Yoon, "A low voltage two axis electromagnetically actuated micromirror with bulk silicon mirror plates and torsion bars," in *Proc. IEEE MEMS Conf.*, Las Vegas, NV, Jan. 2002, pp. 540–543.

[15] I.-J. Cho, T. Song, S.-H. Baek, and E. Yoon, "A low-voltage and low-power RF MEMS switch actuated by combination of electromagnetic and electrostatic forces," in *Proc. 34th Eur. Microwave Conf.*, Amsterdam, The Netherlands, Oct. 2004, pp. 1445–1448.

[16] D. Hyman and M. Harada, "Contact physics of gold microcontacts for MEMS switches," *IEEE Trans. Compon. Packag. Technol.*, vol. 22, no. 3, pp. 357–364, Sep. 1999.

[17] J. Oberhammer and G. Stemme, "Low-voltage high isolation DC-to-RF MEMS switch based on an s-shaped film actuator," *IEEE Trans. Electron Devices*, vol. 51, no. 1, pp. 149–155, Jan. 2004.

[18] J. B. Muldavin and G. M. Rebeiz, "High isolation CPW MEMS shunt switches—Part 1: Modeling," *IEEE Trans. Microw. Theory Tech.*, vol. 48, no. 6, pp. 1045–1052, Jun. 2000.

[19] ——, "Novel series and shunt MEMS switch geometries for X-band applications," in *Proc. 30th Eur. Microwave Conf*, Paris, France, Oct. 2000, pp. 512–515.

Il-Joo Cho received the B.S, M.S., and Ph.D. degrees in electrical engineering from the Korean Advanced Institute of Science and Technology (KAIST), Deajeon, Korea, in 1998, 2000, and 2004, respectively. His doctoral research concerned MEMS micromirrors and RF MEMS switches.

Since 2004, he has been with the LG Electronics Institute of Technology, Seoul, Korea, where he has been involved in the area of MEMS. His research interests include nanodata storage, RF MEMS switches, and bio-MEMS.

Taeksang Song was born in Eumseong, Korea, in 1978. He received the B.S. and M.S. degrees from the Korea Advanced Institute of Science and Technology (KAIST), Deajeon, Korea, in 2000 and 2002, respectively, and is currently working toward the Ph.D. degree at KAIST.

His research interests are RF integrated circuits including voltage-controlled oscillators (VCOs), power amplifiers, and front-ends for disposable wireless sensor networks.

Sang-Hyun Baek was born in Busan, Korea, in 1979. He received the B.S. and M.S. degrees from the Korea Advanced Institute of Science and Technology (KAIST), Deajeon, Korea, in 2001 and 2003, respectively, and is currently working toward the Ph.D. degree at KAIST.

His research interests include the design and implementation of fully integrated low-power transmitters for wireless sensor networks.

Euisik Yoon (S'80–M'82) received the B.S. and M.S. degrees in electronics engineering from Seoul National University, Seoul, Korea, in 1982 and 1984, respectively, and the Ph.D. degree in electrical engineering from The University of Michigan at Ann Arbor, in 1990.

From 1990 to 1994, he was with the Fairchild Research Center, National Semiconductor Corporation, Santa Clara, CA, where he was engaged in research on deep submicrometer CMOS integration and advanced gate dielectrics. From 1994 to 1996, he was a Member of Technical Staff with Silicon Graphics Inc., Mountain View, CA, where he was involved with the design of the MIPS microprocessor R4300i and the RCP three-dimensional (3-D) graphic coprocessor. In 1996, he joined the Department of Electrical Engineering, Korea Advanced Institute of Science and Technology (KAIST), Daejeon, Korea, where he is currently an Associate Professor. His current research interests are MEMS, integrated microsystems, and very large scale integration (VLSI) circuit design.

Dr. Yoon has served on various Technical Program Committees, including the Microprocesses and Nanotechnology Conference, the International Sensor Conference, and the IEEE Asia–Pacific Conference on Application Specific Integrated Circuits (ASICs) Conference. He currently serves the IEEE International Solid-State Circuits Conference (ISSCC) Program Committee and Transducers Technical Program Committee. He was the corecipient of the Student Paper Award presented at the IEEE International Microwave Symposium in 1999 and 2000, respectively.